

# Nano molar level chromogenic and fluorogenic sensing of heavy metal ions using multi-responsive novel Schiff base as a dual mode chemosensor



Prasad G. Mahajan<sup>a</sup>, Nilam C. Dige<sup>b</sup>, Balasaheb D. Vanjare<sup>a</sup>, Eswaran Kamaraj<sup>a</sup>, Sung-Yum Seo<sup>b</sup>, Ki Hwan Lee<sup>a,\*</sup>

<sup>a</sup> Department of Chemistry, Kongju National University, Gongju, Chungnam, 32588, Republic of Korea

<sup>b</sup> Department of Biological Sciences, Kongju National University, Gongju, Chungnam, 32588, Republic of Korea

## ARTICLE INFO

### Keywords:

Schiff base chemosensor  
Fluorescence quenching  
Heavy metal ions  
Naked eye color change  
River water sample

## ABSTRACT

A Schiff base centered chemosensor namely (2*E*,*NE*)-*N*-(2,4-dihydroxybenzylidene)-2-(quinolin-2-ylmethylene)hydrazinocarbothioamide *i.e.* **SB** has been synthesized and further utilized for the selective and sensitive detection of four metal ions through dual channels based on absorption and fluorescence properties. The distinctive recognition of Ni<sup>2+</sup>, Cu<sup>2+</sup>, Co<sup>2+</sup>, and Cd<sup>2+</sup> in an aqueous solution was achieved by observation with the naked eye rapid color change, analyzing the absorption and fluorescence spectrum of chemosensor **SB** in the absence and presence of specific metal ion at respective concentration. The synthesized chemosensor **SB** offered extremely lower detection limit of nano molar level employing either the absorption or fluorescence method. The strong binding constant values such as  $9.02 \times 10^5 \text{ M}^{-1}$  for Ni<sup>2+</sup>,  $11.21 \times 10^5 \text{ M}^{-1}$  for Cu<sup>2+</sup>,  $7.52 \times 10^5 \text{ M}^{-1}$  for Co<sup>2+</sup> and  $6.73 \times 10^5 \text{ M}^{-1}$  for Cd<sup>2+</sup> indicate strong complexation between chemosensor **SB** and respective metal ion. The mechanism for change in the absorption and fluorescence properties of **SB** involves the interaction of respective metal ion with sulfur and oxygen functionality in **SB** molecule followed by the formation of ground state non-fluorescent complex *via* static quenching process. The TD-DFT studies for the theoretical calculations are in support of experimental interpretations. Pleasingly, the present approach allows quantitative determination of said metal ions in water samples at nano molar level.

## 1. Introduction

The current era of the 21<sup>st</sup> century with the massive scale of industrialization and the more than that of scientific technology demand the healthy lifestyle and pollution-free nature for the human being. The industrial boom that mainly concerns with chemical factories and mining projects throughout the world led to damage a peaceful nature which became a threat to the good health of the human being. The ejection of heavy metal ions through such pathways are extremely poisonous, which severely influences the environment and healthy human body [1–3]. Even though some heavy metal ions are crucial in human metabolism and play a pivotal role in the human body, excess intake of such metal ions can be injurious in variety of non-curable complications [4–6]. For this reason, acute quantitative and qualitative detection of such heavy metal ions in an aqueous medium is challenging research task before the scientists working in the fields of sustainable environment sciences.

It is well known that heavy metal ions perform an essential role in the human body as far as several metabolism process and development

is concerned. Amongst the series of heavy metal ions, nickel (Ni<sup>2+</sup>), copper (Cu<sup>2+</sup>), cadmium (Cd<sup>2+</sup>) and cobalt (Co<sup>2+</sup>) are significant metal ions because these are widely used in acting and protecting the particular processes at certain stages in the process of human body or in industrial sections for the production of variety of goods those are useful to the human being [7–10]. For instance, Ni<sup>2+</sup> is nutritionally vital trace metal ion commonly present in a microorganism, plants, and enzymes. However, the excess or low intake of Ni<sup>2+</sup> can disturb the working mechanism at the site which simultaneously affects the respiratory tract, immune system, and disfunction in body portions [7,8]. On the other hand, Cu<sup>2+</sup> is an essential micronutrient for human being and plants. It has a significant role in the processes including metalloenzymes, human nervous system, gene expression, protein functioning, and biological systems of plants. However, neurological disorders such as amyotrophic lateral sclerosis, Parkinson's, Alzheimer's, Wilson's and Menke's diseases may arise due to consumption of a higher dose of Cu<sup>2+</sup> in the human body [10]. Moreover, damage of kidney, anemia, arteriosclerosis and gastrointestinal disorders may be caused by inadequate intake of Cu<sup>2+</sup>. The highly unsafe and carcinogenic

\* Corresponding author.

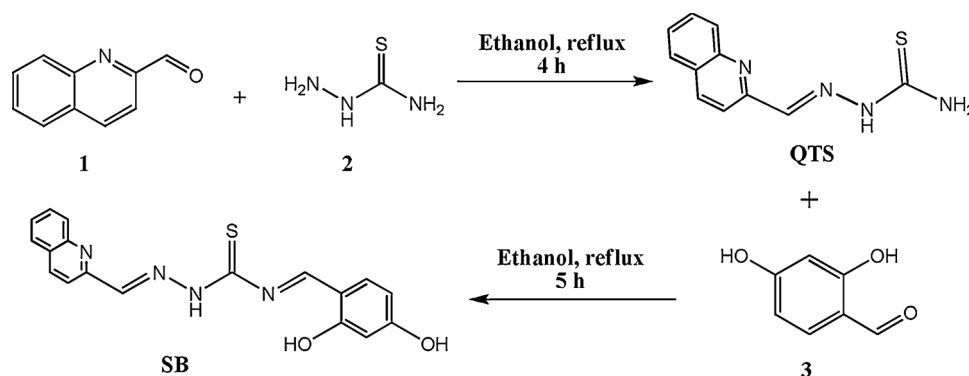
E-mail address: [khlee@kongju.ac.kr](mailto:khlee@kongju.ac.kr) (K.H. Lee).

<https://doi.org/10.1016/j.jphotochem.2019.112089>

Received 26 July 2019; Received in revised form 3 September 2019; Accepted 12 September 2019

Available online 16 September 2019

1010-6030/© 2019 Elsevier B.V. All rights reserved.



Scheme 1. Synthetic approach for the synthesis of compound **SB**.

metal ion widely used in agriculture phosphate fertilizers, electroplated steel, and ceramic enamels in industries is  $\text{Cd}^{2+}$ . The occurrence of toxicity in lungs, bones, kidney, and central nervous system through cancer are some of the damaging causes due to excess consumption of  $\text{Cd}^{2+}$  in human being [8]. Also, an essential element in the nutrition of animals and plants is  $\text{Co}^{2+}$ . The overdose of  $\text{Co}^{2+}$  can produce disorders such as asthma, flushing, and mutilation of thyroid [9]. Therefore, considering the hazardous scenario of said heavy metal ions in ecology, a selective and sensitive method for their independent detection is highly demanded in present day.

Nowadays, several analytical methods and a variety of molecular probes were widely used for the detection of heavy metal ions in aqueous solution. Those molecular probes were specifically based on metalloproteomics, 2, 2'-dihydroxyazobenzene, rhodamine, methylthymol blue complexes on naphthalene, nitrogen doped carbon thin films, mercury embedded oligonucleotide, and luminescent water-soluble CdTe nanowires following the analytical methods such as inductively coupled plasma mass spectroscopy [11], absorption spectroscopy [12], fluorescence spectroscopy [13], atomic absorption spectroscopy [14], voltammetry [15], electrochemical [16] and chemiluminescence [17] processes, respectively. However, each of these proposed methods often offered their own set of either advantages or disadvantages. On the other hand, development in fluorescent based analytical probes which offer naked eye colorimetric detection of more than one heavy metal ions remains an enthusiastic research content in the field of biology, environment samplings, and pharmaceutical chemistry. Considering the ability of thiosemicarbazide to form a chelate with transition metal ions, we aimed to design and synthesize thiosemicarbazide based fluorescent probe. The compounds of thiosemicarbazides are significantly used because of their pharmacological activities and bioinorganic properties [2,18]. The attachment of thiosemicarbazide with suitable fluorophore can develop a fluorescent signaling system when it is in contact with one or more metal ions in the aqueous solution.

In the present research work, we have developed an easy and cost-effective method for the detection of multi-metal ions ( $\text{Ni}^{2+}$ ,  $\text{Cu}^{2+}$ ,  $\text{Cd}^{2+}$  and  $\text{Co}^{2+}$ ) in the aqueous solution using thiosemicarbazone based fluorescent signaling unit. To the best of our knowledge, very few research reports were claimed for the multi-ion recognition assay in the aqueous solution through an optical approach [2,19]. Therefore, it could be the first report, which proposes the independent four metal ions detection present in one aqueous system using fluorescent chemosensor namely (2E,NE)-N-(2-(2,4-dihydroxybenzylidene)-2-(quinolin-2-ylmethylene)hydrazinecarbothioamide) i.e. **SB**. The selectivity order in case of said four metal ions was found to be in order of  $\text{Cu}^{2+} > \text{Ni}^{2+} > \text{Co}^{2+} > \text{Cd}^{2+}$ . The rapid naked eye colorimetric detection, simple operational method, negligible interference of competing metal ions and extremely low detection limit for each metal ion are the advantages of the proposed method. The quantitative determination of  $\text{Ni}^{2+}$ ,  $\text{Cu}^{2+}$ ,  $\text{Cd}^{2+}$ , and  $\text{Co}^{2+}$  from environmental samples collected nearby university is an additional benefit of the proposed

assay.

## 2. Experimental

### 2.1. Materials

The precursors for the synthesis of **SB** were procured from commercial suppliers. Thiosemicarbazide, quinoline 2-carboxaldehyde and 2,4-dihydroxy benzaldehyde were obtained in analytical grade from Sigma-Aldrich, Korea. The solvents such as ethanol and methanol were purchased from Samchun Chemicals, Korea. The double-distilled water was used throughout all experiments.

### 2.2. Methods

The spectral characterization of synthesized compound **SB** was executed by using different analytical techniques such as FT-IR (Frontier IR, Perkin Elmer), NMR (Bruker Avance 400 MHz spectrometer, Germany and  $\text{DMSO}-d_6$  solvent) and GC-MS (2795/ZQ2000, waters) analysis. While optical properties of **SB** in the absence and presence of particular metal ion were investigated with UV-Vis spectrophotometer (UV-2600, Shimadzu, Japan), and fluorescence spectrophotometer (FS-2, Scinco, Korea). Fluorescence lifetime values were obtained using a time-correlated single photon counting (TCSPC) spectrophotometer (HORIBA-iHR320, Japan) employing a nanosecond diode laser operating at its excitation wavelength. The structures of the **SB** and its complexes with respective metal ions i.e.  $\text{Ni}^{2+}$ ,  $\text{Cu}^{2+}$ ,  $\text{Cd}^{2+}$ , and  $\text{Co}^{2+}$  were optimized by TD-DFT using Gaussian 09 software.

### 2.3. Synthesis and spectral characteristics of (2E,NE)-N-(2-(2,4-dihydroxybenzylidene)-2-(quinolin-2-ylmethylene)hydrazinecarbothioamide) i.e. **SB**

The condensation route [2] was employed to synthesize the desired target compound **SB**. Scheme 1 shows two-step synthetic approach for the synthesis of compound **SB**. For this purpose, the first step involves a reaction between quinoline 2-carboxaldehyde **1** (6.3 mmol, 1 g) with thiosemicarbazide **2** (6.3 mmol, 0.58 g) in ethanol at refluxed conditions for 4 h. The progress of the reaction was monitored using TLC techniques. After the completion of the reaction, the mixture was allowed to cool at ambient temperature. The distilled water was added to it and the respective quinoline thiosemicarbazone (**QTS**) was filtered. The practical yield of first step compound was found to be 88.12%. To achieve the synthesis of desired compound **SB**, the second step of the reaction was performed through the reaction of quinoline thiosemicarbazone **QTS** (3.03 mmol, 0.7 g) and 2,4-dihydroxybenzaldehyde **3** (3.03 mmol, 0.42 g) for 5 h in refluxed ethanol followed by monitoring the TLC till the completion of the reaction. The obtained hot solution was allowed to cool and poured on ice-cold water with vigorous stirring. The yellowish colored solid for the desired compound **SB** was

received in 79.68% yield. Yellowish powder; M.P.: 247–249 °C; IR (ESI, Fig. S1): 3750, 3393, 2969, 1738, 1606, 1526, 1501, 1360, 1322, 1260, 1230, 925, 902, 866, 838, 769, 749  $\text{cm}^{-1}$ ;  $^1\text{H-NMR}$ (ESI, Fig. S2, 400 MHz,  $\text{DMSO-}d_6$ ):  $\delta$  11.80 (s, 1H, -NH), 8.47 (s, 1H, -OH), 8.45 (s, 1H, =CH), 8.44 (s, 1H, -OH), 8.37–8.36 (s, 2H, Ar-H,  $J = 4$  Hz), 8.32 (s, 1H, Ar-H), 8.24 (s, 1H, =CH), 7.98–8.02 (q, 2H, Ar-H), 7.76–7.79 (t, 2H, Ar-H,  $J = 4$  & 8 Hz), 7.61–7.64 (t, 2H, Ar-H,  $J = 8$  & 4 Hz) ppm;  $^{13}\text{C-NMR}$ (ESI, Fig. S3, 100 MHz,  $\text{DMSO-}d_6$ ):  $\delta$  179.11, 153.98, 147.98, 143.27, 136.46, 130.60, 129.25, 128.44, 127.70, 118.34 ppm; MS (ESI, Fig. S4): 351 ( $M + 1$ )  $m/z$ . Elemental analysis calcd (%) for  $\text{C}_{18}\text{H}_{14}\text{N}_4\text{O}_2\text{S}$ : C 61.70; H 4.03; N 15.99; O 9.13; S 9.15; found: C 61.68; H 4.04; N 15.99; O 9.14; S 9.15.

#### 2.4. General procedure for the absorption and fluorescence measurements

To examine the characteristic colorimetric and fluorometric sensing of respective metal ion using **SB**, the stock solution of a solvent mixture using methanol and water at 7:3 ratio was prepared. The solution of **SB** ( $5 \times 10^{-5}$  M) in methanol: water (7:3 v/v) system and various metal ions (100 nM) in double-distilled water were prepared. 1 mL stock solution of **SB** was added to 10 mL volumetric flask followed by addition of a known volume of respective metal ion solution (1 mL) and solution of pH 7 (1 mL). Then the series of the solution was diluted up to the mark (10 mL) so that the effective concentration of the metal ion is 10 nM. These solutions were thoroughly shaken, mixed and allowed to keep at room temperature for 10 min. The absorption and fluorescence emission spectra of all these solutions were recorded and compared with the spectra of **SB** as reference. Remarkably, instant naked eye colorimetric alteration was observed for **SB** (colorless) with the addition of respective metal ion viz.  $\text{Ni}^{2+}$  (yellow),  $\text{Cu}^{2+}$  (yellow),  $\text{Cd}^{2+}$  (pale yellow) and  $\text{Co}^{2+}$  (dark yellow) in very short reaction time (3–5 min).

### 3. Results and discussion

#### 3.1. Effect of pH

The pH of solution plays a pivotal role in the performance of any fluorescent chemosensor used for detection of an analyte in aqueous solution. To optimize the best working pH for present fluorescence-based assay, a systematic experiment was carried out in the vicinity of different pH solutions within the range of 1–12. The required solutions were prepared in addition to each pH solution with chemosensor **SB** in a separate test tube and subjected to scan for the fluorescence emission intensity output. Fig. 1 shows the fluorescence intensity response of chemosensor **SB** in different pH solutions. From the results, it was concluded that maximum fluorescence intensity was seen in the pH

range of 6–8. The experiment was repeated three times for consistency, which revealed that the optimization of each solution at pH 7 could be the best choice and ideal condition to perform further experiments. The extreme low (acidic) and high (basic) pH value may disturb the stability of chemosensor in designed methanol: water system and thus decreases fluorescence intensity [20,21]. The effect of pH solutions on fluorescence intensity of chemosensor **SB** in presence of metal ions such as  $\text{Cd}^{2+}$ ,  $\text{Co}^{2+}$ ,  $\text{Ni}^{2+}$ , and  $\text{Cu}^{2+}$  of 10 nM concentration was examined and results are given as Fig. S5 (ESI). This study showed that fluorescence intensity was found to be maximum in the range of pH 6–8 for the complexation between respective metal ion with chemosensor **SB**. This observation led us to conclude that complexation between a metal ion and designed chemosensor **SB** at neutral pH found to be a stable one and most importantly biocompatible for experiments.

#### 3.2. Naked eye colorimetric detection of respective metal ions

The functionalities present in chemosensor **SB** encourage us to select the series of metal ion for the analysis of change in spectral characteristics such as naked eye color change, absorption, and fluorescence response. Initially, chemosensor **SB** in methanol: water (7:3, v/v) was colorless. 1 mL (100 nM) various metal ion solutions viz.  $\text{Ag}^+$ ,  $\text{Na}^+$ ,  $\text{Fe}^{2+}$ ,  $\text{Ni}^{2+}$ ,  $\text{Pb}^{2+}$ ,  $\text{Al}^{3+}$ ,  $\text{Hg}^{2+}$ ,  $\text{Zn}^{2+}$ ,  $\text{Ba}^{2+}$ ,  $\text{Mn}^{2+}$ ,  $\text{Cu}^{2+}$ ,  $\text{NH}_4^+$ ,  $\text{K}^+$ ,  $\text{Ca}^{2+}$ ,  $\text{Mg}^{2+}$ ,  $\text{Cd}^{2+}$ ,  $\text{Cr}^{3+}$ ,  $\text{Co}^{2+}$ , and  $\text{Cr}^{6+}$  of 10 nM was added to chemosensor **SB** ( $5 \times 10^{-5}$  M, 1 mL) and solutions (effective concentration of metal ion was 10 nM) were allowed to stand at ambient temperature. Pleasingly, the color change of solutions was seen within a short reaction time of 3–5 min for respective metal ion from colorless to yellow for  $\text{Ni}^{2+}$  and  $\text{Cu}^{2+}$ , pale yellow for  $\text{Cd}^{2+}$ , and dark yellow for  $\text{Co}^{2+}$  which can easily identify by the naked eye. Fig. 2 shows color change digital photograph of a solution with chemosensor **SB** in the absence and presence of various metal ion. Thus, the present method serves the sensitive and selective color change behavior for multi-ion detection in aqueous solution. This naked-eye colorimetric detection was further supported by studies on absorption and fluorescence characteristics of chemosensor **SB** in the absence and presence of each metal ion.

#### 3.3. Analysis of absorption titration

In order to investigate the discriminating sensing of metal ions in aqueous solution, absorption spectra of chemosensor **SB** ( $5 \times 10^{-6}$  M) was executed in the presence of each metal solution having a concentration of 10 nM. The different metal ion solutions namely  $\text{Ag}^+$ ,  $\text{Na}^+$ ,  $\text{Fe}^{2+}$ ,  $\text{Ni}^{2+}$ ,  $\text{Pb}^{2+}$ ,  $\text{Al}^{3+}$ ,  $\text{Hg}^{2+}$ ,  $\text{Zn}^{2+}$ ,  $\text{Ba}^{2+}$ ,  $\text{Mn}^{2+}$ ,  $\text{Cu}^{2+}$ ,  $\text{NH}_4^+$ ,  $\text{K}^+$ ,  $\text{Ca}^{2+}$ ,  $\text{Mg}^{2+}$ ,  $\text{Cd}^{2+}$ ,  $\text{Cr}^{3+}$ ,  $\text{Co}^{2+}$  and  $\text{Cr}^{6+}$  was used to investigate the effect on absorption properties of chemosensor **SB**. None of the

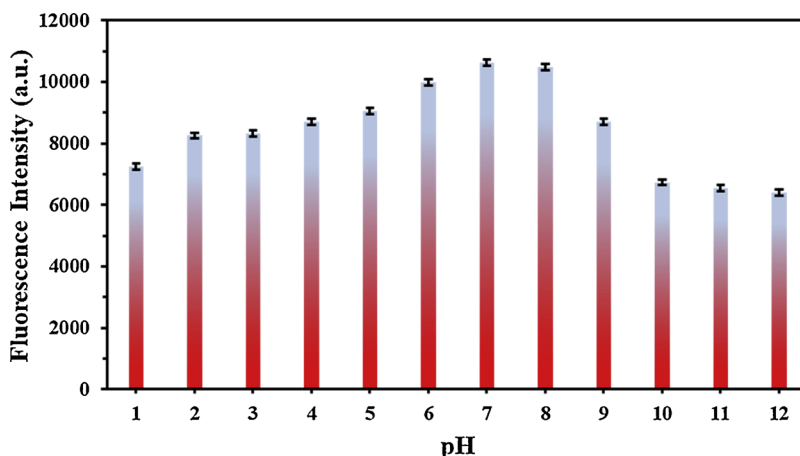


Fig. 1. Fluorescence intensity response of chemosensor **SB** in different pH solutions.

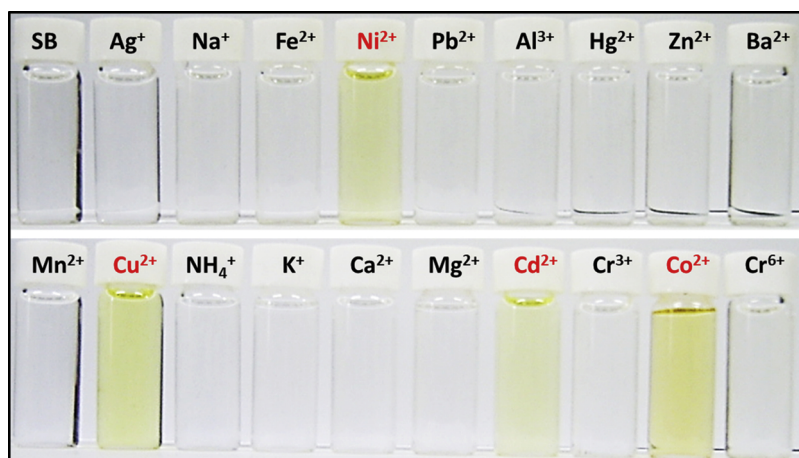


Fig. 2. Digital photograph of solution with chemosensor **SB** in the absence and presence of various metal ion.

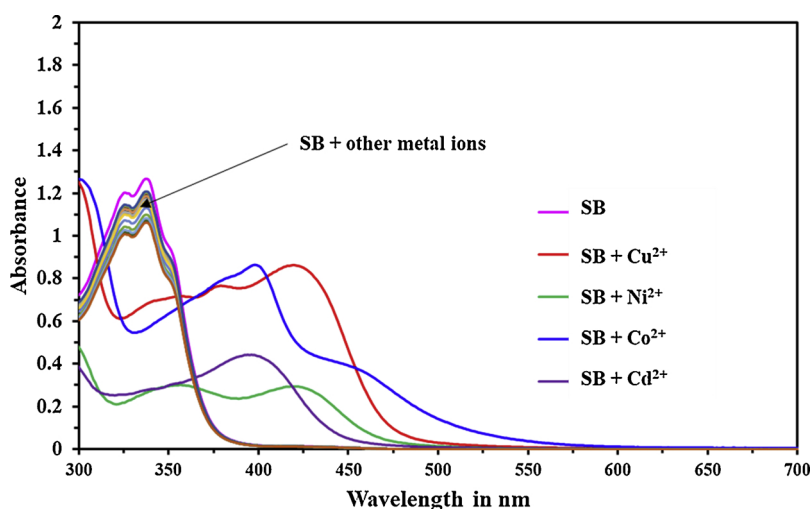


Fig. 3. Absorption spectra of chemosensor **SB** in the absence and presence of various metal ion solutions.

metal ion shows significant absorbance change and any spectral shift for chemosensor **SB** except  $\text{Ni}^{2+}$ ,  $\text{Cd}^{2+}$ ,  $\text{Cu}^{2+}$  and  $\text{Co}^{2+}$ . Fig. 3 shows the absorption spectra of chemosensor **SB** in the absence and presence of various metal ion solutions. It seems that the absorption properties of chemosensor **SB** were considerably changed in terms of absorption intensity and spectral shift. Initially, chemosensor **SB** shows absorption spectrum at 338 nm, which can be assigned to the conjugated  $\pi$  bond system present in the chemosensor structure. The addition of  $\text{Ni}^{2+}$ ,  $\text{Cd}^{2+}$ ,  $\text{Cu}^{2+}$ , and  $\text{Co}^{2+}$  distinctly produce the changes in the absorbance value with a respective bathochromic spectral shift of 84, 61, 86 and 58 nm in the absorption spectrum of chemosensor **SB**. Remarkably, it was observed that the bathochromic spectral shift of four metal ions in absorption spectrum distinguish them from each other and other metal ions too. The studies on spectrophotometric titration of chemosensor **SB** was performed independently with a corresponding metal ion ( $\text{Ni}^{2+}$ ,  $\text{Cd}^{2+}$ ,  $\text{Cu}^{2+}$ , and  $\text{Co}^{2+}$ ) to inspect the effect on absorption properties of chemosensor **SB**. The absorption spectra of chemosensor **SB** in the presence of a variable amount of  $\text{Ni}^{2+}$ ,  $\text{Cd}^{2+}$ ,  $\text{Cu}^{2+}$  and  $\text{Co}^{2+}$  is given as Fig. 4a, b, c, and d, respectively. Figure illustrates that absorption spectra of chemosensor **SB** at 338 nm was decreased along with the appearance of new bathochromically shifted absorption band at their representative wavelength for said metal ions *viz.*  $\text{Ni}^{2+}$ ,  $\text{Cd}^{2+}$ ,  $\text{Cu}^{2+}$  and  $\text{Co}^{2+}$ . The increasing amount of metal ion  $\text{Ni}^{2+}$ ,  $\text{Cd}^{2+}$ ,  $\text{Cu}^{2+}$  and  $\text{Co}^{2+}$  shifts absorption band of chemosensor **SB** from 338 to 422 nm, to 399 nm, to 424 nm and to 396 nm, respectively. The change in absorption value with the addition of an increasing quantity of respective

metal ion solution was also noted. These observations led us to consider that strong interaction might be present in between the respective metal ion ( $\text{Ni}^{2+}$ ,  $\text{Cd}^{2+}$ ,  $\text{Cu}^{2+}$  and  $\text{Co}^{2+}$ ) and functionality such as sulfur (-S) and hydroxyl (-OH) groups in chemosensor **SB**. The digital photographs of the addition of a varying amount of individual metal ion solution to chemosensor **SB** were presented in Fig. 5a, b, c and d for  $\text{Ni}^{2+}$ ,  $\text{Cd}^{2+}$ ,  $\text{Cu}^{2+}$ , and  $\text{Co}^{2+}$ , respectively. All these colorimetric and spectrophotometric results demonstrate that  $\text{Ni}^{2+}$ ,  $\text{Cd}^{2+}$ ,  $\text{Cu}^{2+}$ , and  $\text{Co}^{2+}$  exhibits distinguish properties when in contact with chemosensor **SB** as compared to other metal ion solutions. Hence, such characteristics can be useful to discriminate these four metal ions from each other and a series of metal ion solution at a particular concentration level in sensing applications.

#### 3.4. Analysis of fluorescence titration

The effect of each metal ion on the fluorescence response was studied by executing spectrofluorometric titration. The series of solution containing chemosensor **SB** with and without addition of metal ions (10 nM) such as  $\text{Ag}^+$ ,  $\text{Na}^+$ ,  $\text{Fe}^{2+}$ ,  $\text{Ni}^{2+}$ ,  $\text{Pb}^{2+}$ ,  $\text{Al}^{3+}$ ,  $\text{Hg}^{2+}$ ,  $\text{Zn}^{2+}$ ,  $\text{Ba}^{2+}$ ,  $\text{Mn}^{2+}$ ,  $\text{Cu}^{2+}$ ,  $\text{NH}_4^+$ ,  $\text{K}^+$ ,  $\text{Ca}^{2+}$ ,  $\text{Mg}^{2+}$ ,  $\text{Cd}^{2+}$ ,  $\text{Cr}^{3+}$ ,  $\text{Co}^{2+}$ , and  $\text{Cr}^{6+}$  was examined for change in fluorescence properties. Fig. 6 shows the fluorescence emission spectrum of chemosensor **SB** recorded at its excitation wavelength of 340 nm and in the vicinity of various metal ion solutions having 10 nM concentration. Only  $\text{Ni}^{2+}$ ,  $\text{Cd}^{2+}$ ,  $\text{Cu}^{2+}$  and  $\text{Co}^{2+}$  showed quenching in fluorescence intensity of chemosensor **SB**.

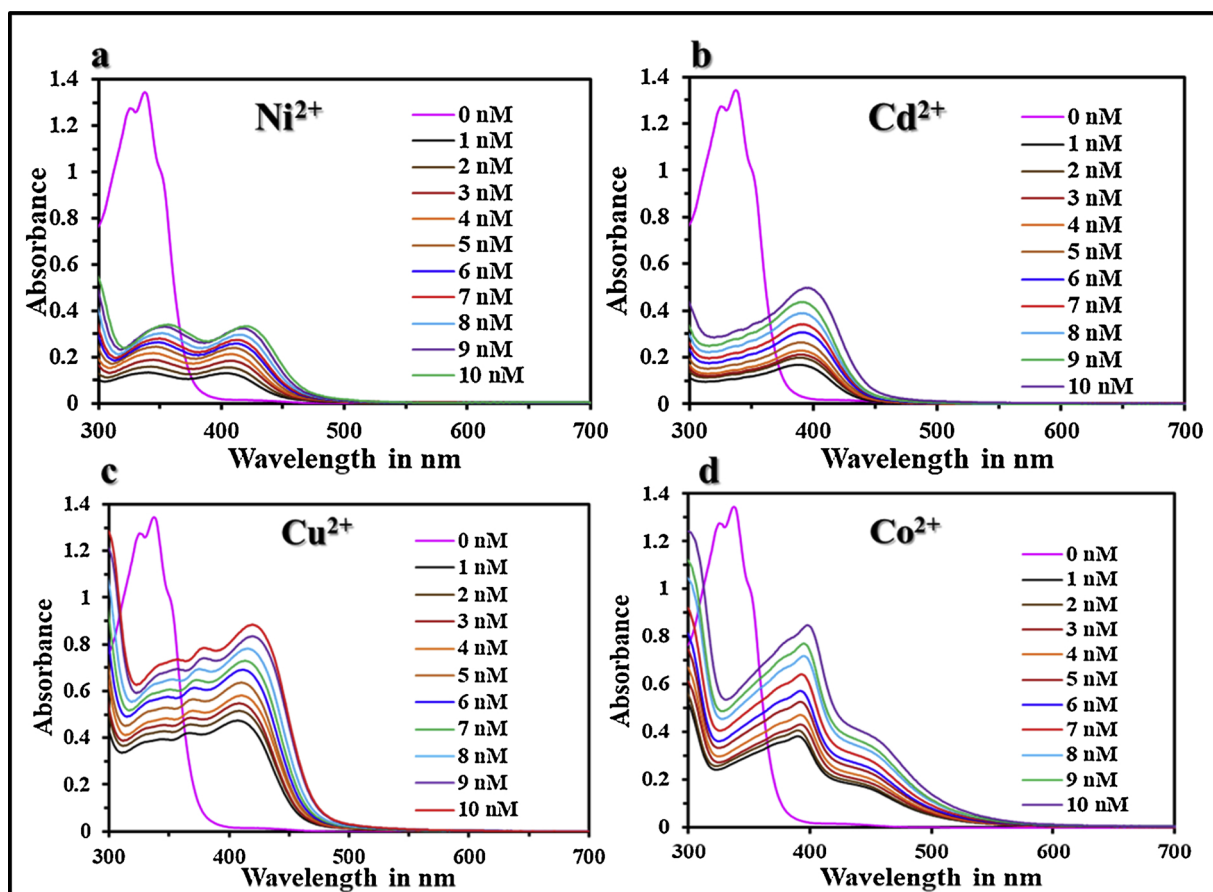


Fig. 4. Absorption titration profiles of chemosensor SB with  $\text{Ni}^{2+}$  (a),  $\text{Cd}^{2+}$  (b),  $\text{Cu}^{2+}$  (c) and  $\text{Co}^{2+}$  (d) at variable concentrations.

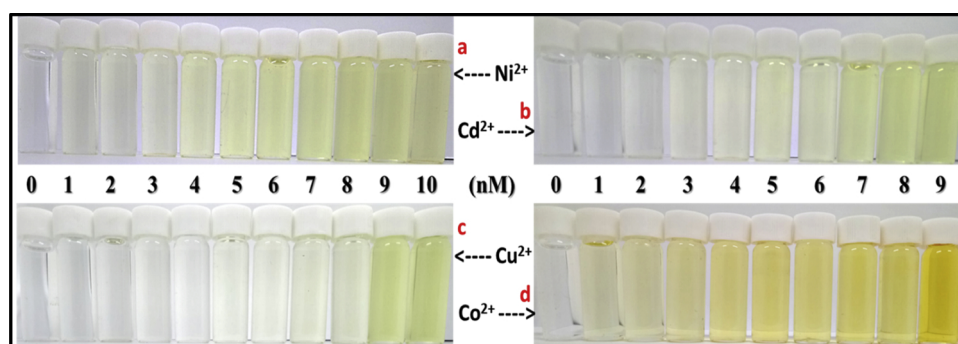


Fig. 5. Digital photographs of addition of varying amount of individual metal ion solution to chemosensor SB.

While other metal ions failed to produce significant change in either way of fluorescence quenching or enhancement of chemosensor SB.  $\text{Cu}^{2+}$  induces 10.5 fold quenching for the initial fluorescence intensity of chemosensor SB among these sensitized four metal ions. However, other metal ions  $\text{Ni}^{2+}$ ,  $\text{Co}^{2+}$  and  $\text{Cd}^{2+}$  introduced 9.2, 8.6 and 8.1 fold fluorescence quenching to the original value of chemosensor SB, respectively. These observations led us to consider that strong complexation between chemosensor SB and representative metal ion through -S (sulfur) and -O (oxygen) may responsible for the fluorescence quenching process. The ability of strong complex formation through binding of chemosensor and the metal ion is found to be in the order of  $\text{SB-Cu}^{2+} > \text{SB-Ni}^{2+} > \text{SB-Co}^{2+} > \text{SB-Cd}^{2+}$ .

### 3.5. Effect of foreign metal ions

The successful sensor application of any fluorescent chemosensor

can be achieved by systematically minimizing or eliminating the effect of foreign metal ions present in the same aqueous system. Hence, in order to investigate the effect of foreign metal ions on the binding ability and fluorescence response, simple spectrophotometric titration was performed followed by recording the emission spectrum of each solution under studies. The fluorescence emission spectrum of chemosensor SB was recorded in the presence of  $\text{Ni}^{2+}$ ,  $\text{Cd}^{2+}$ ,  $\text{Cu}^{2+}$ , and  $\text{Co}^{2+}$  (10 nM) separately. The equimolar concentration (10 nM) of foreign metal ions such as  $\text{Ag}^+$ ,  $\text{Na}^+$ ,  $\text{Fe}^{2+}$ ,  $\text{Pb}^{2+}$ ,  $\text{Al}^{3+}$ ,  $\text{Hg}^{2+}$ ,  $\text{Zn}^{2+}$ ,  $\text{Ba}^{2+}$ ,  $\text{Mn}^{2+}$ ,  $\text{NH}_4^+$ ,  $\text{K}^+$ ,  $\text{Ca}^{2+}$ ,  $\text{Mg}^{2+}$ ,  $\text{Cr}^{3+}$ , and  $\text{Cr}^{6+}$  was added in composite holding the solution of chemosensor SB and respective metal to examine the change in fluorescence response. Fig. 7a indicates quenching of fluorescence by the addition of  $\text{Cd}^{2+}$  was affected by addition of  $\text{Co}^{2+}$ ,  $\text{Ni}^{2+}$ , and  $\text{Cu}^{2+}$  while remaining metal ions do not affect the output. The most pronounced effect on fluorescence intensity was seen in case of  $\text{Co}^{2+}$  about 8.5 fold,  $\text{Ni}^{2+}$  about 9.1 fold and  $\text{Cu}^{2+}$

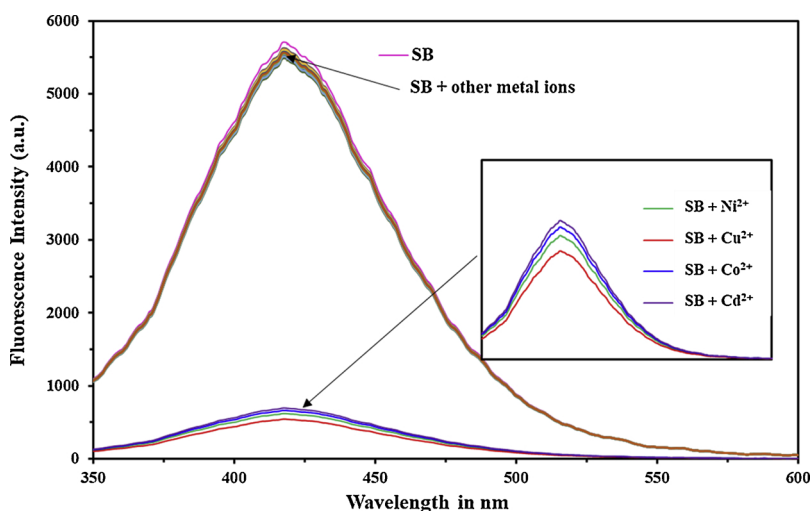


Fig. 6. Fluorescence emission spectrum of chemosensor **SB** in the vicinity of various metal ion solutions [10 nM] recorded at  $\lambda_{ex} = 340$  nm.

about 10.4 fold which were significant features of respective metal ions when subjected to independent fluorescence titration. Further, Fig. 7b illustrates that only  $Ni^{2+}$  and  $Cu^{2+}$  ions affect the fluorescence intensity quenched by  $Co^{2+}$  to chemosensor **SB**. It was noted that 9.2 fold and 10.4 fold quenching seen in case of addition of  $Ni^{2+}$  and  $Cu^{2+}$  ions to composite holding chemosensor **SB** and  $Co^{2+}$  solution. Nevertheless, almost all metal ions exhibit a negligible effect on fluorescence intensity of chemosensor **SB** quenched by  $Ni^{2+}$  except  $Cu^{2+}$  as presented in Fig. 7c. The equimolar addition of  $Cu^{2+}$  to the same solution containing chemosensor **SB** and  $Ni^{2+}$  introduce immediate 10.5 fold fluorescence quenching in initial value which is characteristics property posed by  $Cu^{2+}$  ion seen during fluorescence titration experiment. In contrast, Fig. 7d shows all metal ion solutions failed to affect the fluorescence intensity induced by the addition of  $Cu^{2+}$  to chemosensor **SB**. These results reveal that chemosensor **SB** possesses strong binding affinity

towards metal ions in the ascending order as  $Cd^{2+} < Co^{2+} < Ni^{2+} < Cu^{2+}$ . This means that  $Cu^{2+}$  can expel out the other metal ion from their respective complex with chemosensor **SB**. Furthermore,  $Ni^{2+}$  can remove  $Co^{2+}$  and  $Cd^{2+}$  from their complex with **SB**. In addition,  $Co^{2+}$  can able to remove only  $Cd^{2+}$  metal ion from their respective complex with **SB**. This selective and sensitive behavior can be utilizing and quantitatively analyzing to discriminate these four metal ions in aqueous solution. Satisfyingly, these results indicate the stability order of respective metal ion with chemosensor **SB** to be  $SB-Cu^{2+} > SB-Ni^{2+} > SB-Co^{2+} > SB-Cd^{2+}$ , which was further supported by evaluation of binding parameters and computational analysis through time-dependent density functional theory (TD-DFT). Scheme 2 illustrates schematic interpretation for plausible competing sensing behavior of designed chemosensor **SB** towards  $Ni^{2+}$ ,  $Cd^{2+}$ ,  $Cu^{2+}$  and  $Co^{2+}$  ion. Further, all these experimental observations imply the

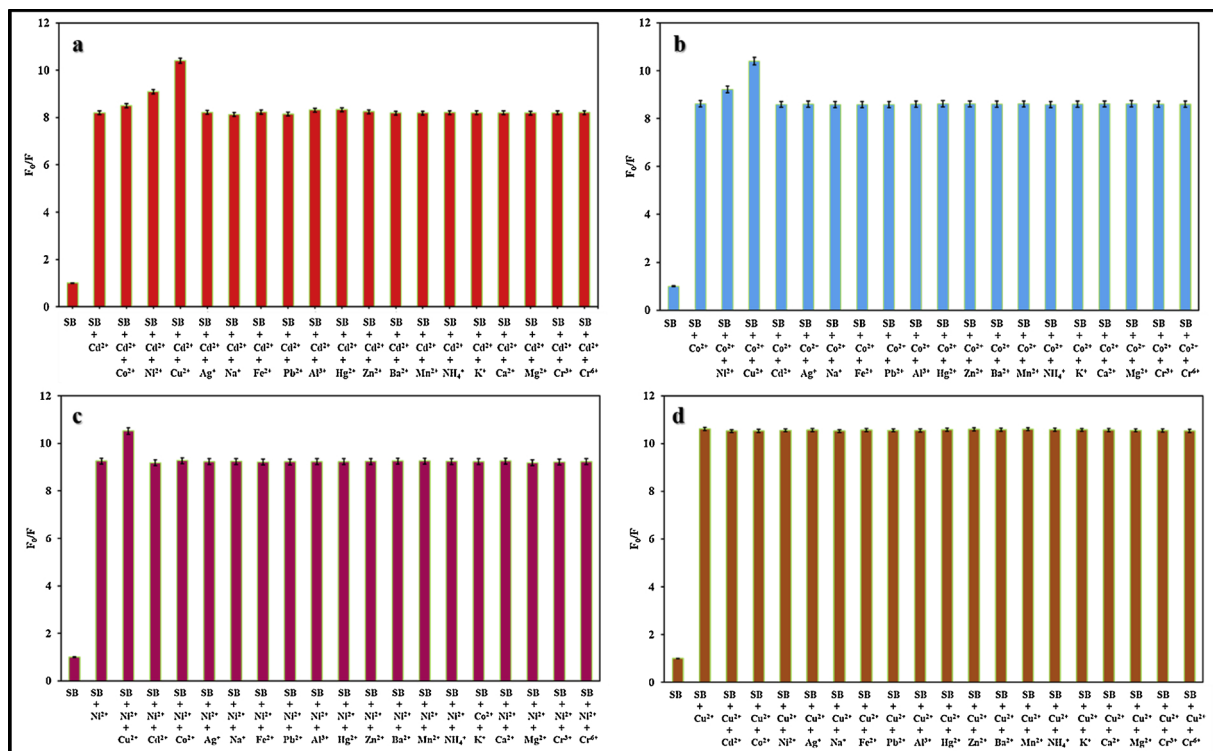
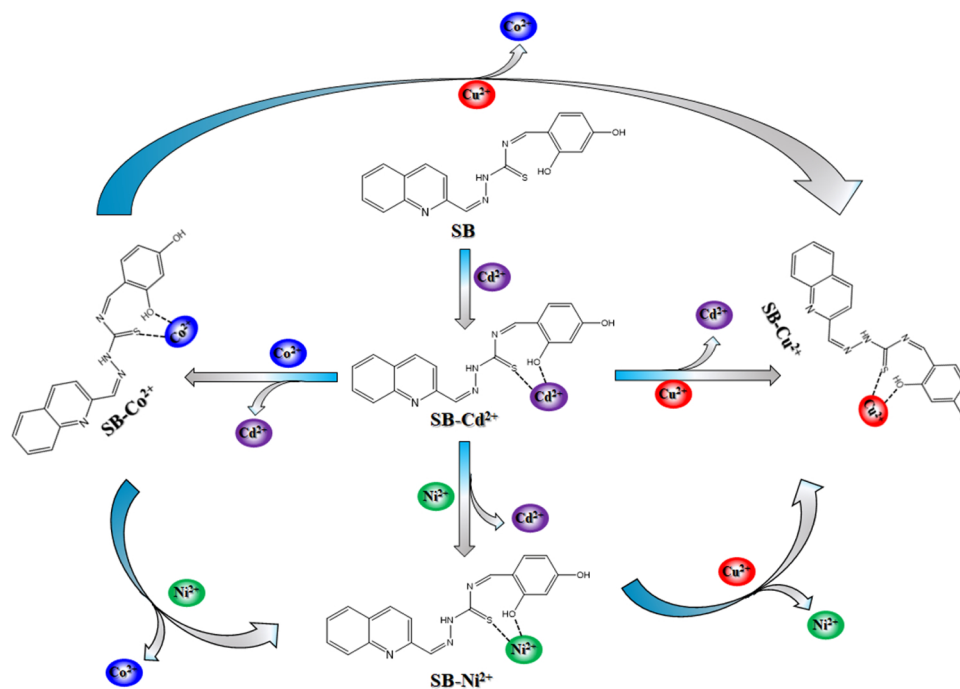


Fig. 7. Effect of foreign metal ions on detections of respective metal ions –  $Cd^{2+}$  (a),  $Co^{2+}$  (b),  $Ni^{2+}$  (c) and  $Cu^{2+}$  (d).



**Scheme 2.** Schematic interpretation for plausible competing sensing behavior of designed chemosensor **SB** towards  $\text{Ni}^{2+}$ ,  $\text{Cd}^{2+}$ ,  $\text{Cu}^{2+}$  and  $\text{Co}^{2+}$  ion.

maximum stability for the formed complexes with chemosensor **SB** by the Irving William stability order which deals with the divalent first-row transition metal ions [22]. According to the Irving William stability order, the stability of complexes formed by divalent first-row transition metal ions generally increase across the period and found to be resemblance in present investigations as  $\text{SB-Cu}^{2+} > \text{SB-Ni}^{2+} > \text{SB-Co}^{2+}$  excluding  $\text{SB-Cd}^{2+}$ .

### 3.6. Evaluation of binding parameters

To investigate the binding stoichiometry between chemosensor **SB** and representative metal ion, Job's method [23–25] was utilized. In this method, the sum of concentration of the specific metal ion and chemosensor **SB** was kept constant followed by variation in the only mole fraction of metal ion under studied from 0.1 to 0.9. The Job's plot derived from fluorescence and absorption output for respective metal ions shown in Fig. 8a-d. From the figure, it seems that absorbance and fluorescence emission intensity reached maximum when mole fraction of each metal ion found to be 0.5. This observation concludes that interaction mode of specific metal ion *i.e.*  $\text{Ni}^{2+}$ ,  $\text{Cd}^{2+}$ ,  $\text{Cu}^{2+}$ , and  $\text{Co}^{2+}$  with chemosensor **SB** results in 1:1 binding stoichiometry. In addition, binding constant was evaluated using modified Benesi-Hildebrand (B-H) equation based on fluorescence output. Eq. (1) given below is known as modified Benesi-Hildebrand (B-H) equation [26–28] used to estimate the binding constant ( $K_B$ ) of complexation between chemosensor **SB** and specific metal ion under study.

$$\frac{1}{F_0 - F} = \frac{1}{(F_0 - F_m)} + \frac{1}{K_B(F_0 - F_m)} \frac{1}{[M^{2+}]^n} \quad (1)$$

where,  $F_m$ ,  $F_0$ , and  $F$  denotes the minimum fluorescence intensity of chemosensor **SB** with metal ion, initial fluorescence intensity and fluorescence intensity at respective concentration for the metal ion under studies, respectively. The number of metal ion bound per chemosensor **SB** unit is represented as 'n'. The modified Benesi-Hildebrand (B-H) plot is given as Fig. 9a-d for representative metal ions. Figure illustrates a straight line nature with respective slope values. The estimated value of binding constant for each metal ion  $\text{Ni}^{2+}$ ,  $\text{Cd}^{2+}$ ,  $\text{Cu}^{2+}$ , and  $\text{Co}^{2+}$  with chemosensor **SB** was calculated and given in Table 1. The higher binding constant value indicates the strong and efficient

binding between target metal ion and chemosensor **SB**. From these calculations, it was concluded that chemosensor **SB** forms most stable complex with  $\text{Cu}^{2+}$  and least stable complex with  $\text{Cd}^{2+}$ , whereas other metal ions  $\text{Ni}^{2+}$  and  $\text{Co}^{2+}$  shows comparative complexation with characteristics binding constant value. The binding between functional groups having -S and -O atom in chemosensor **SB** with respective metal ion was examined by performing IR and  $^1\text{H}$  NMR titrations. Figs. 10 and 11 illustrate the results for the IR and  $^1\text{H}$  NMR titration between chemosensor **SB** and metal ion (1:1 equivalent) under studies, respectively. The experiment for IR titration (Fig. 10) clearly indicates the disappearance of stretching frequencies of -OH ( $3750\text{ cm}^{-1}$ ) and -C = S ( $1225\text{ cm}^{-1}$ ) functional groups when respective metal ion is in contact with the chemosensor **SB**. This observation proves the interactions between -S and -O atoms in chemosensor **SB** with a metal ion. Furthermore,  $^1\text{H}$  NMR titrations also supports the interaction pattern at -S and -O site of chemosensor **SB**. Fig. 11 shows a partially expanded  $^1\text{H}$  NMR spectrum of chemosensor **SB** along with the addition of respective metal ion. The appearance of two singlets at  $\delta$  8.44 and 8.47 in  $^1\text{H}$  NMR spectrum of chemosensor **SB** (Fig. 11a) were assigned to protons belongs to -OH at ortho position (\*) and -OH at para position (\*\*\*) of phenyl ring, respectively. The addition of metal ion  $\text{Cu}^{2+}$ ,  $\text{Ni}^{2+}$ ,  $\text{Co}^{2+}$  and  $\text{Cd}^{2+}$  (Fig. 11b-e) to equivalent quantity of chemosensor **SB** clearly shows the absence of one -OH peak at  $\delta$  8.47 along with a shift in  $\delta$  value for aromatic and other protons present in the compound. The full and partially expanded spectrum for the  $^1\text{H}$  NMR titrations between chemosensor **SB** and the metal ion is given as supporting information (Figs. S6-S9, ESI).

### 3.7. Stern-Volmer plot and limit of detection

The fluorometric titration was carried out for the examination of consequent change in the fluorescence intensity of chemosensor **SB** with the incremental addition of a specific metal ion solution within the range of 0–10 nM. Fig. 12a-d shows fluorescence quenching of chemosensor **SB** with the addition of  $\text{Ni}^{2+}$ ,  $\text{Cu}^{2+}$ ,  $\text{Co}^{2+}$ , and  $\text{Cd}^{2+}$  for the concentration of 0–10 nM, respectively. Figures illustrate that the fluorescence intensity of chemosensor **SB** decreases regularly without any spectral shift when in contact with target metal ion. The

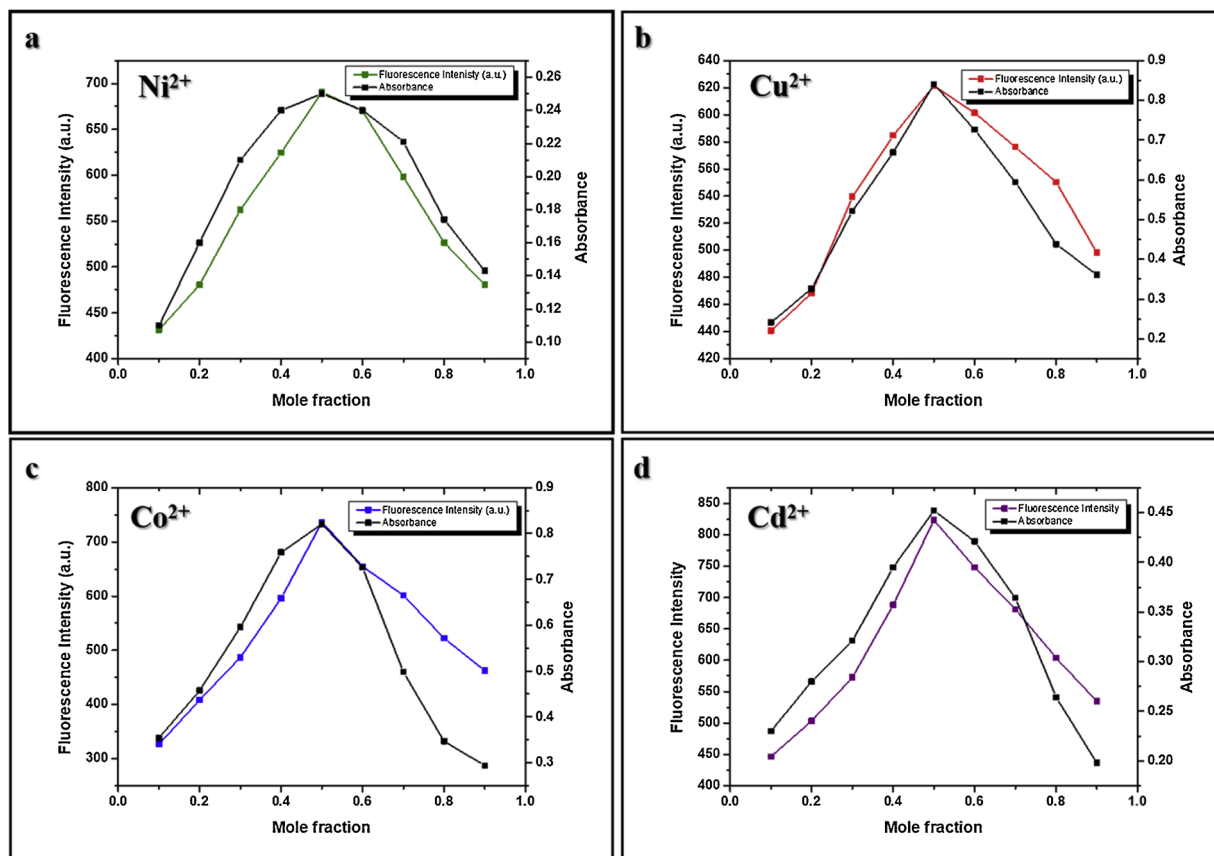


Fig. 8. Job's plot derived from fluorescence and absorption output for respective metal ions.

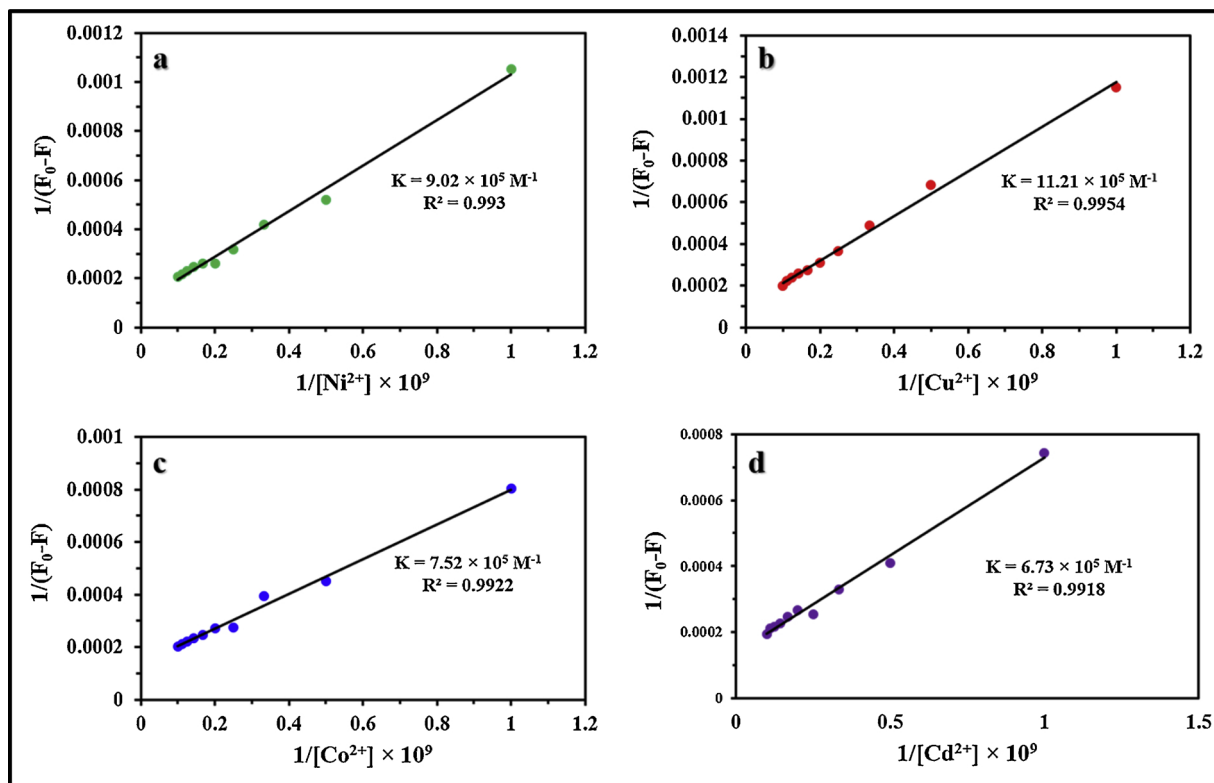
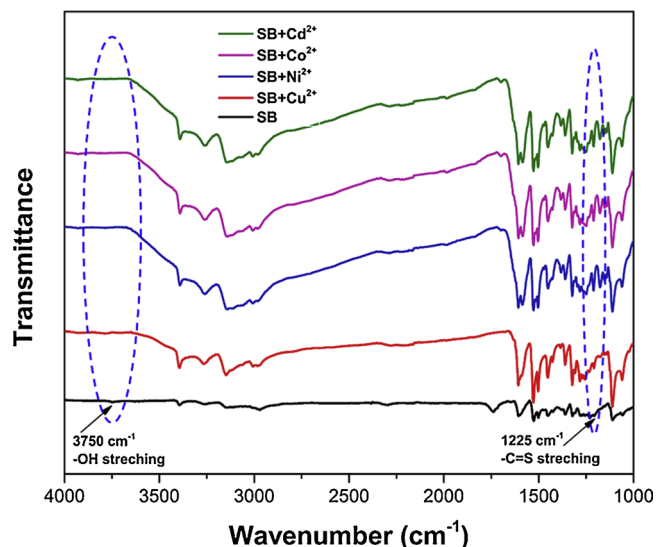


Fig. 9. Modified Benesi-Hildebrand (B-H) plot for representative metal ions.

**Table 1**  
Estimated binding constant, Stern-Volmer constant and Limit of detection values for chemosensor **SB** with respective metal ion.

Metal ion	Binding constant (K) $\times 10^5 \text{ M}^{-1}$	Stern-Volmer constant ( $K_{sv}$ ) $\times 10^8 \text{ M}^{-1}$	Limit of detection (LOD) in nM	
			via absorption	Via fluorescence
Ni <sup>2+</sup>	9.02	4.94	0.656	0.637
Cu <sup>2+</sup>	11.21	5.27	0.224	0.184
Co <sup>2+</sup>	7.52	4.17	1.047	1.053
Cd <sup>2+</sup>	6.73	3.82	1.043	1.070



**Fig. 10.** IR spectrum of chemosensor **SB** without and with addition of respective metal ion (1:1 equivalent).

fluorescence quenching data was subjected to analyzed for the evaluation of fluorescence quenching efficiency through conventional the Stern-Volmer equation. It was evaluated by the Stern-Volmer plot [29–31] using Eq. (2),

$$\frac{F_0}{F} = 1 + K_{sv}[Q] \quad (2)$$

Where,  $F_0$ ,  $F$ , and  $K_{sv}$  represents initial fluorescence intensity of chemosensor **SB**, the fluorescence intensity of chemosensor **SB** after the addition of a particular concentration of quencher  $[Q]$  and the Stern-Volmer constant, respectively. Fig. 13a–d shows the Stern-Volmer plot for each metal ion understudies with chemosensor **SB**. The values of Stern-Volmer constant for metal ions such as Ni<sup>2+</sup>, Cd<sup>2+</sup>, Cu<sup>2+</sup>, and Co<sup>2+</sup> with chemosensor **SB** are given in Table 1. Further, absorption titration was carried out with and without the addition of an increasing amount of metal ion (0–10 nM) to the solution containing chemosensor **SB**. Fig. 4a–d demonstrates consistent raise in absorption value of chemosensor **SB** with the addition 0–10 nM of Ni<sup>2+</sup>, Cd<sup>2+</sup>, Cu<sup>2+</sup> and Co<sup>2+</sup>, respectively. The absorption titration profiles were used to plot the changes in the absorbance value versus specific concentration of the metal ion. Fig. S10a–d (ESI) served as a calibration plot based on absorption titrations for chemosensor **SB** with the addition of Ni<sup>2+</sup>, Cd<sup>2+</sup>, Cu<sup>2+</sup> and Co<sup>2+</sup>, respectively. Fig. 13a–d and Fig. S10a–d (supporting information, ESI) were used as calibration plots for the estimation of limit of detection (LOD) for corresponding metal ions based on fluorescence and absorption method, respectively. The limit of detection (LOD) [32–34] for said metal ions was calculated using Eq. (3) and given in Table 1.

$$\text{LOD} = \frac{3.3\sigma}{K} \quad (3)$$

Where, standard deviation and slope of the calibration curve denoted by  $\sigma$  and  $K$ , respectively. The comparatively analogous LOD values for Ni<sup>2+</sup>, Cd<sup>2+</sup>, Cu<sup>2+</sup> and Co<sup>2+</sup> metal ion through both methods (fluorescence and absorption) signifies its selectivity and sensitivity towards detection approach. The obtained values of LOD were extremely lower than that of the LOD values reported by other methods for these metal ions. The comparison syntax between obtained LOD value using proposed analytical approach and LOD value claimed by previous reports for these representative metal ions namely Cd<sup>2+</sup>, Co<sup>2+</sup>, Ni<sup>2+</sup>, and Cu<sup>2+</sup> is given as supporting information (Tables S1–S4, ESI).

### 3.8. Mechanism of fluorescence quenching of **SB** by respective metal ions

The functional groups having hetero atoms -S and -O are responsible to interact with the respective metal ion results in changes for absorption and fluorescence properties of chemosensor **SB**. The studies on the effect of foreign metal addition to the solution containing chemosensor **SB** and specific metal ion reveals that Cu<sup>2+</sup> imposed strong interaction with chemosensor **SB**. Meanwhile, other metals show weak and strong interactions in comparison to each other. The plausible interaction of metal ion and chemosensor **SB** results in decreasing the radiative pathways from its excited state and further quenching in fluorescence [35]. Scheme 2 illustrates the binding nature of chemosensor **SB** with target metal ion responsible for the fluorescence quenching process. The nature of fluorescence quenching process was investigated by experimental observations of absorption titration, the Stern-Volmer plot and estimation of fluorescence lifetime values in the absence and presence of metal ion in the solution of chemosensor **SB**. The absorption titration profiles (Fig. 4) indicates a change in maximum absorption wavelength to longer wavelength with the addition of various concentration of the metal ion. Also, observation of the linear Stern-Volmer plot (Fig. 13) for each metal ion understudies indicates the nature of fluorescence quenching process can be static rather than dynamic. The fluorescence quenching process is static when the interaction between chemosensor and analyte must occur at ground state levels. To support our conclusion of static type fluorescence quenching process, estimation of fluorescence lifetime was employed. If the interaction between chemosensor and analyte is static, then fluorescence life remains constant even if variation in concentration of analyte molecule and vice-versa for dynamic type [29,33,36,37]. This is because of contribution to the lifetime comes only from the unassociated fluorescent probe once in contact with analyte molecule [29,33]. The average fluorescence lifetime values of chemosensor **SB** with and without the addition of particular metal ions solutions having specific concentration given as Table 2. In the present investigation, the fluorescence lifetime value of chemosensor **SB** with and without the addition of target molecules remains unchanged which clearly signifies the nature of fluorescence quenching process was purely static. The formation of a non-fluorescent complex between chemosensor **SB** and metal ion at ground state follows a static quenching process. In this process, the complex of chemosensor **SB** with metal ion absorbs the energy from light followed by immediate returns to ground state without photon emission results in fluorescence quenching. Scheme 3 illustrates a pictorial presentation of static type fluorescence quenching of chemosensor **SB** with a particular metal ion.

### 3.9. Computational analysis through Time-dependent density functional theory (TD-DFT)

The studies on theoretical calculations were performed through a computational approach based on time-dependent density functional theory (TD-DFT) using the Gaussian 09 program [38]. This study was accessed to determine the coordination behavior and investigate the theoretical characteristics of chemosensor **SB** and its complexation with metal ions viz. Ni<sup>2+</sup>, Cd<sup>2+</sup>, Cu<sup>2+</sup> and Co<sup>2+</sup>. The Becke-3-Lee-Yang-Parr (B3LYP) functional and lan12dz basis set was used to

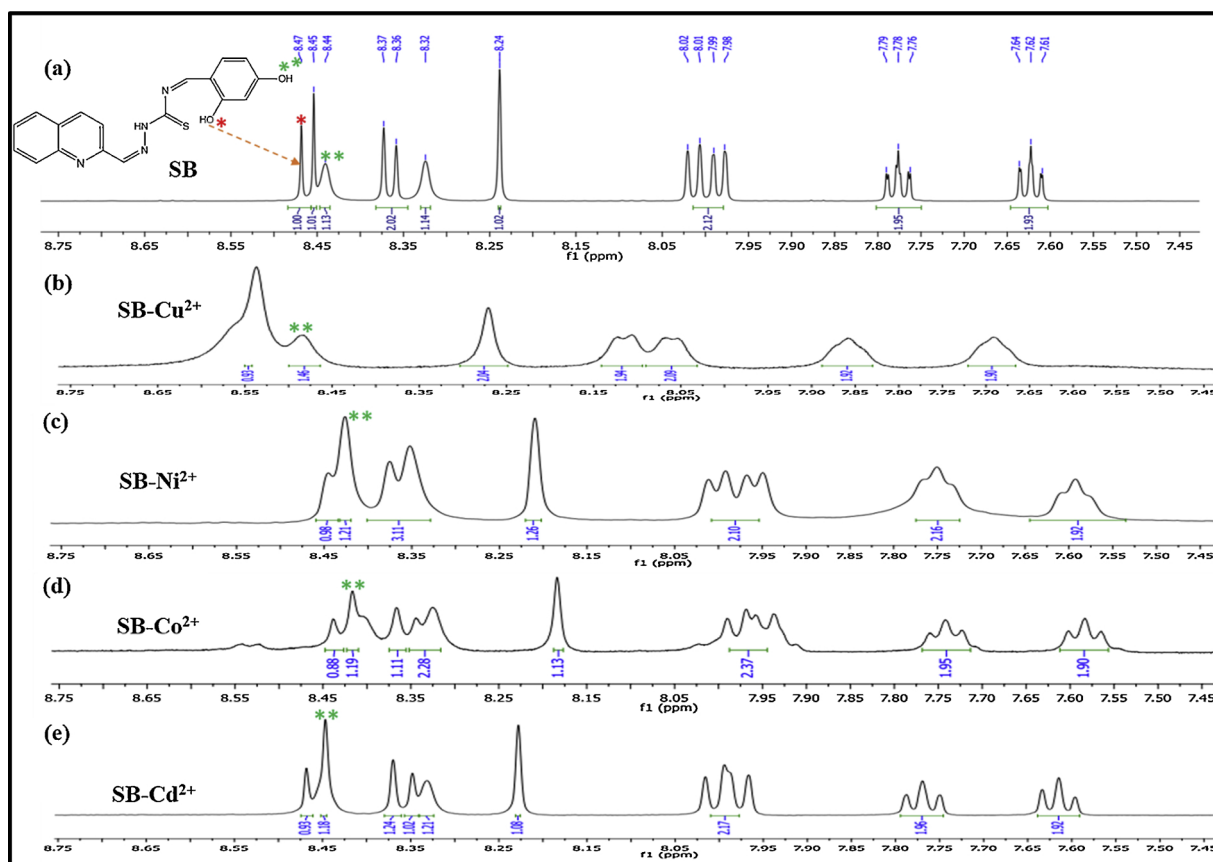


Fig. 11.  $^1\text{H}$  NMR titration of chemosensor SB with respective metal ion (1:1 equivalent) in  $\text{DMSO}-d_6$ .

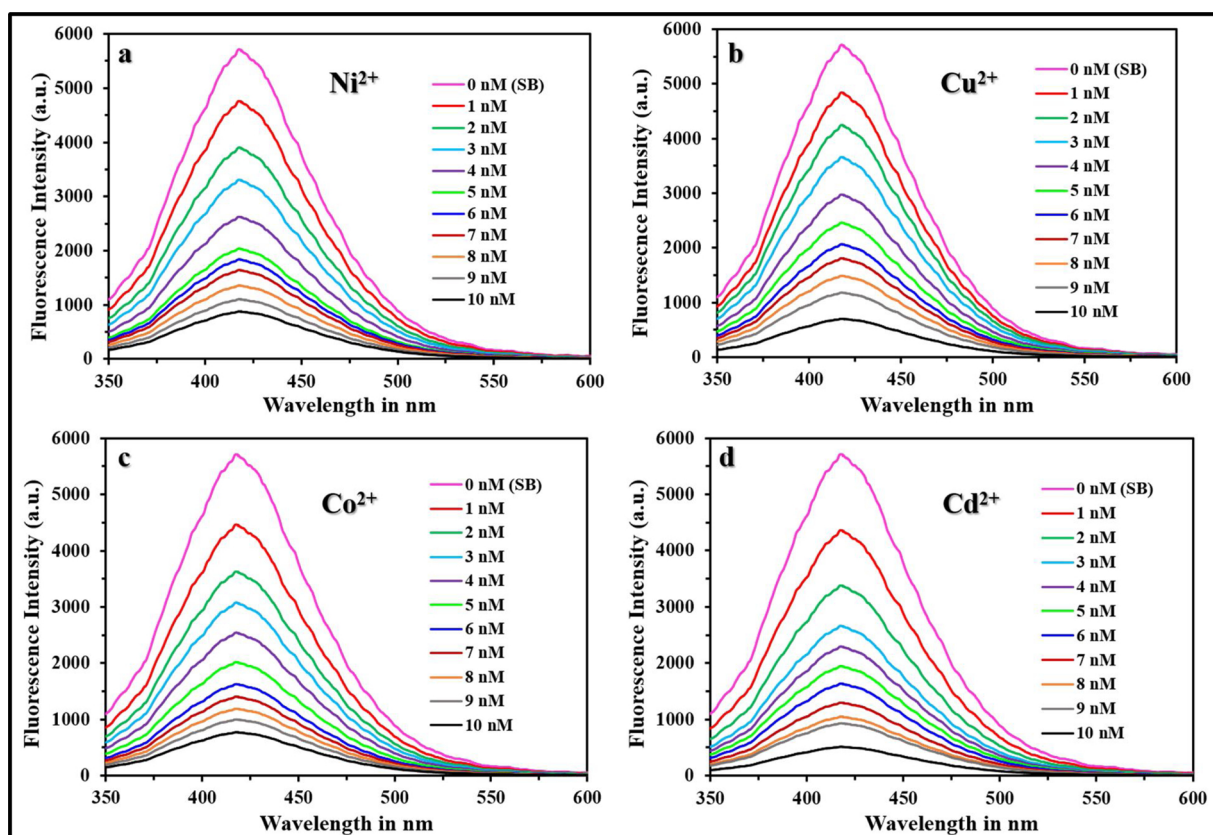


Fig. 12. Fluorescence quenching of chemosensor SB with addition of  $\text{Ni}^{2+}$  (a),  $\text{Cu}^{2+}$  (b),  $\text{Co}^{2+}$  (c) and  $\text{Cd}^{2+}$  (d) within the concentration range of 0–10 nM.

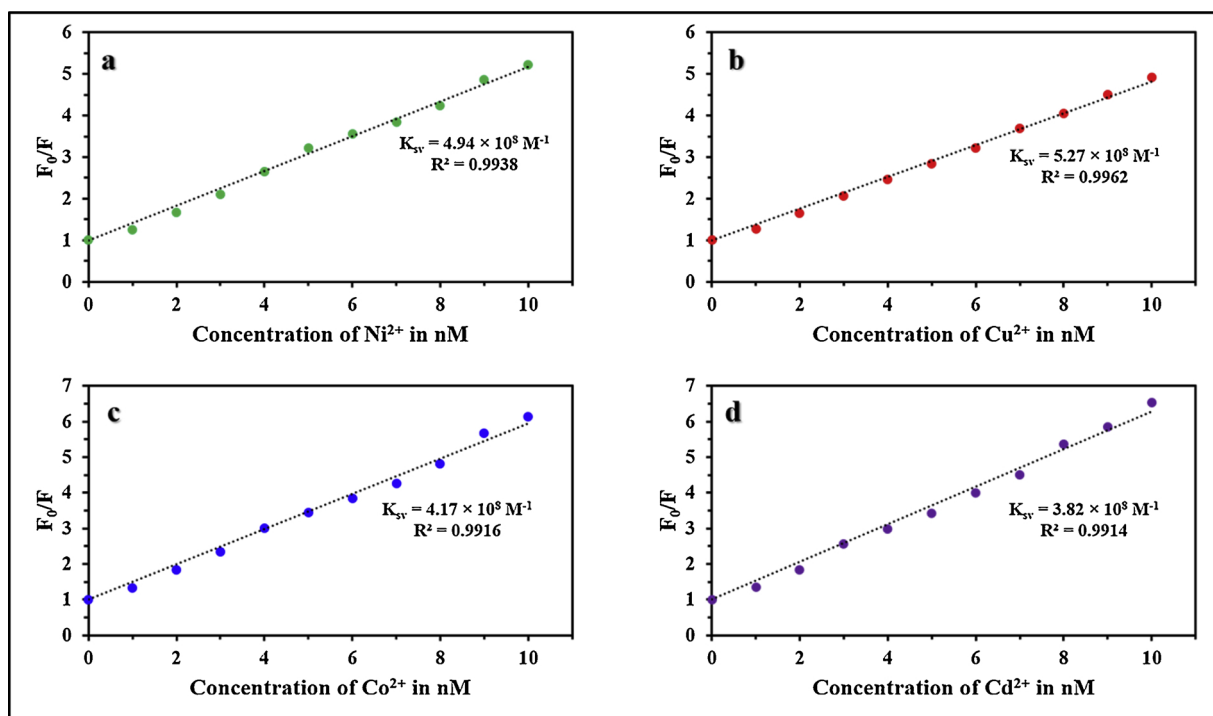


Fig. 13. Stern-Volmer plot for each metal ion under studied with chemosensor SB.

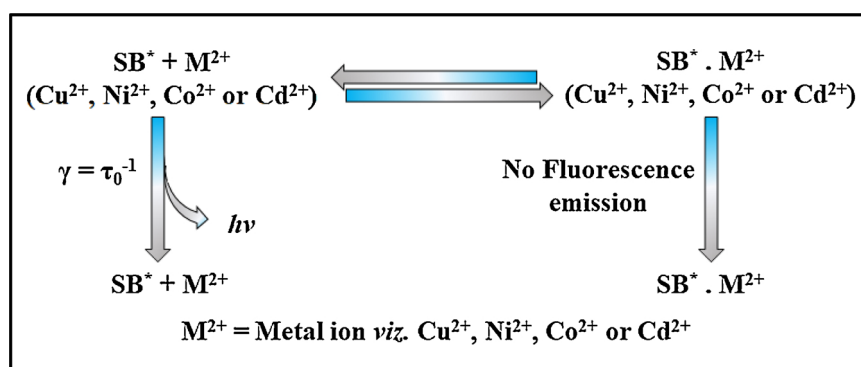
Table 2

Fluorescence lifetime values of chemosensor SB with addition of target metal ion at particular concentration.

Concentration of Metal ion added (nM)	Fluorescence lifetime value of SB ( $\tau$ ) after addition of metal ion (ns)			
	Ni <sup>2+</sup>	Cu <sup>2+</sup>	Co <sup>2+</sup>	Cd <sup>2+</sup>
0	4.61	4.61	4.61	4.61
4	4.62	4.62	4.64	4.66
6	4.59	4.64	4.63	4.62
10	4.58	4.61	4.60	4.57

optimize the structures of target complexes of metal ions with compound SB. The calculated energy-optimized stable structures along with the plausible mode of the binding interaction between chemosensor SB and each metal ion under studies are shown in Fig. 14, which characterizes electron distribution of highest occupied molecular orbital (HOMO) and lowest unoccupied molecular orbital (LUMO) energy levels of chemosensor SB and its complexation with the respective metal ion. Fig. 14 shows HOMO-LUMO diagram of chemosensor SB in which the electron distribution of HOMO is mainly over the dihydroxybenzyl-

thiosemicarbazone backbone, while the LUMO is primarily over the quinoline part. The HOMO side of chemosensor SB provides the most binding impact for metal ions. The changes in HOMO-LUMO energies occurred due to the complexation between chemosensor SB and respective metal ion. The strong electrostatic interactions *via* functional groups posing hetero atoms like -S and -O of chemosensor SB was accountable to form complex with metal ions. The energy values of HOMOs and LUMOs for corresponding complex and free chemosensor SB are given in Table 3. It was found that the energy values of HOMOs and LUMOs for the complexed form were lower than that of chemosensor SB. The higher stability of complexed form of chemosensor SB with metal ions was concluded by observing the lower values of total energies of complexed form than free SB. Thus, TD-DFT calculations imply the complex with lower stabilization energy will have higher stability. In the present case, the decreasing order of stabilization energy for the complexes of metal ions with chemosensor SB are found to be SB-Cd<sup>2+</sup> > SB-Co<sup>2+</sup> > SB-Ni<sup>2+</sup> > SB-Cu<sup>2+</sup>. While, the increasing stability order for complexes are found to be in the order of SB-Cd<sup>2+</sup> < SB-Co<sup>2+</sup> < SB-Ni<sup>2+</sup> < SB-Cu<sup>2+</sup>. Hence, these observations are in support of our experimental observations during absorption and fluorescence studies.



Scheme 3. Pictorial presentation of static type fluorescence quenching of chemosensor SB with particular metal ion.

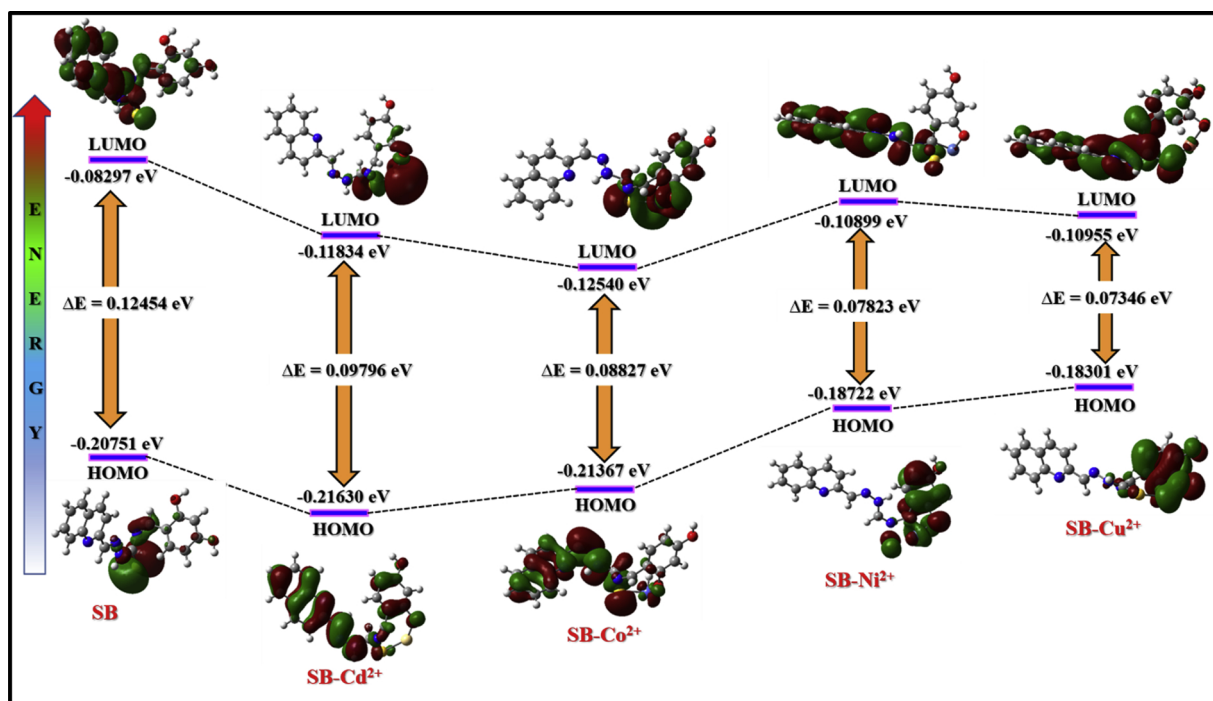


Fig. 14. Electron distribution of highest occupied molecular orbital (HOMO) and lowest unoccupied molecular orbital (LUMO) energy levels of chemosensor **SB** and its complexation with respective metal ion.

Table 3

Comparison syntax of theoretical HOMO-LUMO energies of chemosensor **SB** in the absence and presence of individual metal ions.

Chemosensor System	Energy of HOMO (eV)	Energy of LUMO (eV)	ΔE (eV)
SB	-0.20751	-0.08297	0.12454
SB-Cd <sup>2+</sup>	-0.21630	-0.11834	0.09796
SB-Co <sup>2+</sup>	-0.21367	-0.12540	0.08827
SB-Ni <sup>2+</sup>	-0.18722	-0.10899	0.07823
SB-Cu <sup>2+</sup>	-0.18301	-0.10955	0.07346

### 3.10. Application of proposed fluorescence quenching method for river water sample analysis

The successful demonstration of developed fluorescence-based analytical method for the quantitative determination of metal ions in aqueous solution is a key factor of the present study. The real water sample was collected from a local river near the university for applying the proposed method. The collected sample was filtered and boiled to avoid the solid impurities and dissolved gases if any. The target solutions have been prepared by spiking the standard respective each metal ion (Ni<sup>2+</sup>, Cu<sup>2+</sup>, Cd<sup>2+</sup>, and Co<sup>2+</sup>) with particular concentration levels to the solution of chemosensor **SB** and diluted by collected river sample. Thus, Fig. 13a-d was used as a calibration curve to estimate the recovery of a spiked quantity of respective metal ion. The investigated outcomes thus obtained for each metal ion is presented in Tables 4 and 5. From the results, it is clear that the observed experimental values fell

Table 4

Quantitative determination of spiked quantity of Cd<sup>2+</sup> and Co<sup>2+</sup> in the river sample using proposed method.

Samples Studied	Amount of standard Cd <sup>2+</sup> ion added (nM)	Total Cd <sup>2+</sup> ion found (nM) (n = 3)	Recovery of added Cd <sup>2+</sup> ions (%)	Amount of standard Co <sup>2+</sup> ion added (nM)	Total Co <sup>2+</sup> ion found (nM) (n = 3)	Recovery of added Co <sup>2+</sup> ions (%)
River water	3	2.98	99.33	3	2.99	99.66
	6	5.99	99.83	6	5.99	99.83
	9	8.98	99.77	9	8.97	99.66

\*n = Average of three determinations.

within the very close range of expected values. This research observation highlights the selectivity, sensitivity, swift and naked-eye colorimetric methodology for the fluorescence-based quantitative estimation of four heavy metal ions in aqueous solution using chemosensor **SB**.

## 4. Conclusions

The selective and sensitive detection of four metal ions at one time was successfully achieved by using Schiff base as chemosensor **SB**. Amongst the tested series of metal ion in the aqueous solution, chemosensor **SB** showed sensitive response towards only Ni<sup>2+</sup>, Cu<sup>2+</sup>, Cd<sup>2+</sup>, and Co<sup>2+</sup>. The selective binding ability of the metal ion with chemosensor **SB** was found to be in the order of Cu<sup>2+</sup>, Ni<sup>2+</sup>, Co<sup>2+</sup> and then Cd<sup>2+</sup>. The effect of foreign analytes on the performance of present analytical approach was performed and discussed in detail. The stoichiometry between chemosensor and respective metal ion was evaluated by using Job's method. In the meantime, the binding constant was estimated by plotting fluorescence output based on the modified Benesi-Hilderbrand equation. The absorption studies offer the detection limit of 0.224 nM, 0.656 nM, 1.047 nM and 1.043 nM for Cu<sup>2+</sup>, Ni<sup>2+</sup>, Co<sup>2+</sup>, and Cd<sup>2+</sup>, respectively. Meanwhile, limit of detection through the fluorescence method for Cu<sup>2+</sup>, Ni<sup>2+</sup>, Co<sup>2+</sup> and Cd<sup>2+</sup> was found to be 0.184 nM, 0.637 nM, 1.053 nM and 1.070 nM, respectively. The sensitive and selective detection of said metal ions was demonstrated through absorption spectrum, fluorescence spectrum, interference studies, estimation of fluorescence lifetime and TD-DFT calculations. The plausible complexation mode and binding interaction of chemosensor

**Table 5**  
Quantitative determination of spiked quantity of Ni<sup>2+</sup> and Cu<sup>2+</sup> in the river sample using proposed method.

Samples Studied	Amount of standard Ni <sup>2+</sup> ion added (nM)	Total Ni <sup>2+</sup> ion found (nM) (n = 3)	Recovery of added Ni <sup>2+</sup> ions (%)	Amount of standard Cu <sup>2+</sup> ion added (nM)	Total Cu <sup>2+</sup> ion found (nM) (n = 3)	Recovery of added Cu <sup>2+</sup> ions (%)
River water	3	2.97	99.00	3	2.99	99.66
	6	5.99	99.83	6	5.98	99.66
	9	8.99	99.88	9	8.99	99.88

\*n = Average of three determinations.

SB with respective metal ion were supported by IR and <sup>1</sup>H NMR titrations. The prospective application of designed chemosensor SB involves the quantitative determination of said metal ion in water samples at nano molar concentration. Hence, all the experimental and theoretical results distinctly revealed that designed Schiff base centered chemosensor SB offers a modern approach for the detection of Cu<sup>2+</sup>, Ni<sup>2+</sup>, Co<sup>2+</sup>, and Cd<sup>2+</sup> metal ions in aqueous solution through either absorption or fluorescence method.

### Declaration of Competing Interest

Authors declares no conflict of interest.

### Acknowledgements

This research was supported by Basic Science Research Program through the National Research Foundation of Korea(NRF) funded by the Ministry of Education(NRF- 2019R1I1A3A01059089).

### Appendix A. Supplementary data

Supplementary material related to this article can be found, in the online version, at doi:<https://doi.org/10.1016/j.jphotochem.2019.112089>.

### References

- (a) S. Paul, S. Bhuyan, S.K. Mukhopadhyay, N.C. Murmu, P. Banerjee, Sensitive and selective in vitro recognition of biologically toxic As(III) by rhodamine based chemoreceptor, ACS Sustainable Chem. Eng. (2019), <https://doi.org/10.1021/acsschemeng.9b00935>;
- (b) S.M.Z. Hossain, J.D. Brennan, B-galactosidase-Based colorimetric paper sensor for determination of heavy metals, Anal. Chem. 83 (2011) 8772–8778.
- S. Sarkar, T. Mondal, S. Roy, R. Saha, A.K. Ghosh, S.S. Panja, A multi-responsive thiosemicarbazone-based probe for detection and discrimination of group 12 metal ions and its application in logic gates, New J. Chem. 42 (2018) 15157–15169.
- P. Patnaik, Handbook of Environmental Analysis: Chemical Pollutants in Air, Water, Soil and Solid Wastes vol. 69, CRC Press, Boca Raton, FL, 1997.
- A. Singh, Metal poisoning, Dream 2047 (17) (2015) 32–33.
- P. Pohl, Determination of metal content in honey by atomic absorption and emission spectrometries, Trac-Trend. Anal. Chem. 28 (2009) 117–128.
- (a) B. Valeur, I. Leray, Design principles of fluorescent molecular sensors for cation recognition, Coord. Chem. Rev. 205 (2000) 3–40;
- (b) A. Baker, Fluorescence excitation-emission matrix characterization of some sewage-impacted rivers, Environ. Sci. Technol. 35 (2001) 948–953.
- (a) Q. Han, Y. Huo, L. Yang, X. Yang, Y. He, J. Wu, Determination of trace nickel in water samples by graphite furnace atomic absorption spectrometry after mixed micelle-mediated cloud point extraction, Molecules 23 (2018) 2597 doi:10.3390/molecules23102597;
- (b) J.J. Scott Fordsmand, Toxicity of nickel to soil organisms in Denmark, Rev. Environ. Contam. Toxicol. 148 (1997) 1–34;
- (c) V. Bencko, Nickel: A review of its occupational and environmental toxicology, J. Hyg. Epidem. Micro. Immun. 27 (1983) 237–247.
- (a) G.G.V. Kumar, M.P. Kesavan, M. Sankarganesh, K. Sakthipandi, J. Rajesh, G. Sivaraman, A Schiff base receptor as a fluorescence turn-on sensor for Ni<sup>2+</sup> ions in living cells and logic gate application, New J. Chem. (2018), pp. 2865–2873;
- (b) E.L. Silva, P.S. Roldan, M.F. Giné, Simultaneous preconcentration of copper, zinc, cadmium, and nickel in water samples by cloud point extraction using 4-(2-pyridylazo)-resorcinol and their determination by inductively coupled plasma optical emission spectrometry, J. Hazard. Mater. (2009), pp. 1133–1138;
- (c) J.B. Sullivan, G.R. Krieger, Clinical Environmental Health and Toxic Exposures, 2nd ed., Lippincott Williams & Wilkins, 2001.
- (a) M. Yang, J.B. Chae, C. Kim, R.G. Harrison, A visible chemosensor based on carbonylhydrazide for Fe(II), Co(II) and Cu(II) in aqueous solution, Photochem. Photobiol. Sci. 18 (2019) 1249–1258;
- (b) S.A. El-Safty, Functionalized hexagonal mesoporous silica monoliths with hydrophobic azo-chromophore for enhanced Co(II) ion monitoring, Adsorption 15 (2009) 227–239;
- (c) M. Gharehbaghi, F. Shemirani, M.D. Farahani, Cold-induced aggregation microextraction based on ionic liquids and fiber optic-linear array detection spectrophotometry of cobalt in water samples, J. Hazard. Mater. 165 (2009) 1049–1055.
- (a) A. Mondal, A.R. Chowdhury, S. Bhuyan, S.K. Mukhopadhyay, P. Banerjee, A simple urea-based multianalyte and multichannel chemosensor for the selective detection of F<sup>-</sup>, Hg<sup>2+</sup> and Cu<sup>2+</sup> in solution and cells and the extraction of Hg<sup>2+</sup> and Cu<sup>2+</sup> from real water sources: a logic gate mimic ensemble, Dalton Trans. 48 (2019) 4375–4386;
- (b) Y. Wang, H.Q. Chang, W.N. Wu, W.B. Peng, Y.F. Yan, C.M. He, T.T. Chen, X.L. Zhao, Z.Q. Xu, Rhodamine 6G hydrazone bearing pyrrole unit: ratiometric and selective fluorescent sensor for Cu<sup>2+</sup> based on two different approaches, Sens. Actuators B 228 (2016) 395–400;
- (c) L. Zhang, X. Zhang, A selectively fluorescein-based colorimetric probe for detecting copper(II) ion. Spectrochim. Acta A: molec. Biomol. Spectroscopy 133 (2014) 54–59;
- (d) S. Paul, P. Ghosh, S. Bhuyan, S.K. Mukhopadhyay, P. Banerjee, Nanomolar-level selective dual channel sensing of Cu<sup>2+</sup> and CN<sup>-</sup> from an aqueous medium by an opto-electronic chemoreceptor, Dalton Trans. 47 (2018) 1082–1091.
- I. Tomalova, P. Foltynova, V. Kanicky, J. Preisler, MALDI MS and ICP MS detection of a single CE separation record: a tool for metalloproteomics, Anal. Chem. 86 (2014) 647–654.
- H. Liu, H. Zhao, Z. Tong, Y. Zhang, B. Lan, J. Wang, A colorimetric, ratiometric, and fluorescent cobalt(II) chemosensor based on mixed organic ligands, Sensors Actuators B Chem. 239 (2017) 511–514.
- (a) S. Wang, H. Ding, Y. Wang, C. Fan, Y. Tu, G. Liu, S. Pu, An “off-on-off” sensor for sequential detection of Cu<sup>2+</sup> and hydrogen sulfide based on a naphthalimide-rhodamine B derivative and its application in dual-channel cell imaging, RSC Adv. 8 (2018) 33121–33128;
- (b) X. Wang, J. Tao, X. Chen, H. Yang, An ultrasensitive and selective “off-on” rhodamine-based colorimetric and fluorescent chemodosimeter for the detection of Cu<sup>2+</sup>, Sens. Actuators B 244 (2017) 709–716.
- N. Pourreza, R. Hoveizavi, Simultaneous preconcentration of Cu, Fe and Pb as methylthymol blue complexes on naphthalene adsorption and flame atomic absorption determination, Anal. Chim. Acta 549 (2005) 124–128.
- N.W. Khun, E. Liu, Linear sweep anodic stripping voltammetry of heavy metals from nitrogen doped tetrahedral amorphous carbon thin films, Electrochim. Acta 54 (2009) 2890–2898.
- Z.Q. Zhu, Y.Y. Su, J. Li, D. Li, J. Zhang, S.P. Song, Y. Zhao, G.X. Li, C.H. Fan, Highly sensitive electrochemical sensor for mercury(II) ions by using a mercury-specific oligonucleotide probe and gold nanoparticle-based amplification, Anal. Chem. 81 (2009) 7660–7666.
- B. Tang, J.Y. Niu, C.G. Yu, L.H. Zhuo, J.C. Ge, Highly luminescent water-soluble Cd Te nanowires as fluorescent probe to detect copper (II), Chem. Commun. (33) (2005) 4184–4186.
- P.G. Mahajan, N.C. Dige, B.D. Vanjare, H. Raza, M. Hassan, S.Y. Seo, C.H. Kim, K.H. Lee, Synthesis and biological evaluation of 1,2,4-triazolidine-3-thiones as potent acetyl-cholinesterase inhibitors: in vitro and in silico analysis through kinetics, chemoinformatics and computational approaches, Mol. Divers. (2019), <https://doi.org/10.1007/s11030-019-09983-y>.
- M. Banerjee, M. Ghosh, S. Ta, J. Das, D. Das, A smart optical probe for detection and discrimination of Zn<sup>2+</sup>, Cd<sup>2+</sup> and Hg<sup>2+</sup> at nano-molar level in real samples, J. Photochem. Photobiol. 377 (2019) 286–297.
- B.D. Vanjare, P.G. Mahajan, S.K. Hong, K.H. Lee, Discriminating chemosensor for detection of Fe<sup>3+</sup> in aqueous media by fluorescence quenching methodology, Bull. Korean Chem. Soc. 39 (2018) 631–637.
- J. Lyklema, Fundamentals of Interface and Colloid Science, Elsevier, Wageningen, 1995.
- H.M.N.H. Irving, R.J.P. Williams, The stability of transition-metal complexes, J. Chem. Soc. (1953) 3192–3210.
- P. Job, Formation and stability of inorganic complexes in solution, Ann. Chim. 9 (1928) 113–203.
- J.M. Jung, S.Y. Lee, E. Nam, M.H. Lim, C. Kim, A highly selective turn-on chemosensor for Zn<sup>2+</sup> in aqueous media and living cells, Sensors Actuators B Chem. 244 (2017) 1045–1053.
- P.G. Mahajan, N.C. Dige, B.D. Vanjare, S.H. Eo, S.J. Kim, K.H. Lee, A nano sensor for sensitive and selective detection of Cu<sup>2+</sup> based on fluorescein: cell imaging and drinking water analysis, Spectrochim. Acta A. Mol. Biomol. Spectrosc. 216 (2019) 105–116.
- P.G. Mahajan, D.P. Bhopate, G.B. Kolekar, S.R. Patil, N-methyl isatin nanoparticles

- as a novel probe for selective detection of  $\text{Cd}^{2+}$  ion in aqueous medium based on chelation enhanced fluorescence and application to environmental sample, *Sens. Actuators B Chem.* 220 (2015) 864–872.
- [27] A. Samanta, N. Guchhait, S.C. Bhattacharya, A simple but highly selective and sensitive fluorescence reporter for toxic Cd (II) ion via excimer formation, *Chem. Phys. Lett.* 612 (2014) 251–255.
- [28] H.A. Benesi, J.H. Hildebrand, A spectrophotometric investigation of the interaction of iodine with aromatic hydrocarbons, *J. Am. Chem. Soc.* 71 (1949) 2703–2707.
- [29] P.G. Mahajan, D.P. Bhopate, A.A. Kamble, D.K. Dalavi, G.B. Kolekar, S.R. Patil, Selective sensing of  $\text{Fe}^{2+}$  ions in aqueous solution based on fluorescence quenching of SDS capped rubrene nanoparticles: application in pharmaceutical formulation, *Anal. Methods* 7 (2015) 7889–7898.
- [30] P.G. Mahajan, N.K. Desai, D.K. Dalavi, D.P. Bhopate, G.B. Kolekar, S.R. Patil, Cetyltrimethylammonium bromide capped 9-Anthraldehyde nanoparticles for selective recognition of phosphate anion in aqueous solution based on fluorescence quenching and application for analysis of chloroquine, *J. Fluoresc.* 25 (2015) 31–38.
- [31] P.G. Mahajan, G.B. Kolekar, S.R. Patil, Recognition of D-Penicillamine using schiff base centered fluorescent organic nanoparticles and application to medicine analysis, *J. Fluoresc.* 27 (2017) 829–839.
- [32] G.L. Long, J.D. Winefordner, Limit of detection a closer look at the IUPAC definition, *Anal. Chem.* 55 (1983) 712A–724A.
- [33] (a) P.G. Mahajan, N.C. Dige, B.D. Vanjare, Y. Han, S.J. Kim, S.K. Hong, K.H. Lee, Intracellular imaging of zinc ion in living cells by fluorescein based organic nanoparticles, *Sens. Actuators B Chem.* 267 (2018) 119–128; (b) P.G. Mahajan, N.C. Dige, N.K. Desai, S.R. Patil, V.V. Kondalkar, S.K. Hong, K.H. Lee, Selective detection of  $\text{Co}^{2+}$  by fluorescent nano probe: diagnostic approach for analysis of environmental samples and biological activities, *Spectrochim. Acta A. Mol. Biomol. Spectrosc.* 198 (2018) 136–144.
- [34] (a) P.G. Mahajan, G.B. Kolekar, S.R. Patil, Fluorescence-based logic gate for sensing of  $\text{Ca}^{2+}$  and  $\text{F}^-$  ions using PVP crowned chrysenes nanoparticles in aqueous medium, *Luminescence* 32 (2017) 845–854; (b) K.S. Patil, P.G. Mahajan, S.R. Patil, Fluorimetric detection of  $\text{Sn}^{2+}$  ion in aqueous medium using Salicylaldehyde based nanoparticles and application to natural samples analysis, *Spectrochim. Acta A. Mol. Biomol. Spectrosc.* 170 (2017) 131–137.
- [35] D.P. Bhopate, P.G. Mahajan, K.M. Garadkar, G.B. Kolekar, S.R. Patil, Polyvinyl pyrrolidone capped fluorescent anthracene nanoparticles for sensing fluorescein sodium in aqueous solution and analytical application for ophthalmic samples, *Luminescence* 30 (2015) 1055–1063.
- [36] M.K. Seery, N. Fay, T. McCormac, E. Dempsey, R.J. Forster, T.E. Keyes, Photophysics of ruthenium polypyridyl complexes formed with lacunary polyoxotungstates with iron addenda, *Phys. Chem. Chem. Phys.* 7 (2005) 3426–3433.
- [37] Y.K. Kim, R.C. Johnson, J.T. Hup, Gold nanoparticle-based sensing of “spectroscopically silent” heavy metal ions, *Nano Lett.* 1 (2001) 165–167.
- [38] M.J. Frisch, G.W. Trucks, H.B. Schlegel, G.E. Scuseria, M.A. Robb, J.R. Cheeseman, G. Scalmani, V. Barone, B. Mennucci, G.A. Petersson, H. Nakatsuji, M. Caricato, X. Li, H.P. Hratchian, A.F. Izmaylov, J. Bloino, G. Zheng, J.L. Sonnenberg, M. Hada, M. Ehara, K. Toyota, R. Fukuda, J. Hasegawa, M. Ishida, T. Nakajima, Y. Honda, O. Kitao, H. Nakai, T. Vreven, J.A. Montgomery Jr., J.E. Peralta, F. Ogliaro, M. Bearpark, J.J. Heyd, E. Brothers, K.N. Kudin, V.N. Staroverov, R. Kobayashi, J. Normand, K. Raghavachari, A. Rendell, J.C. Burant, S.S. Iyengar, J. Tomasi, M. Cossi, N. Rega, J.M. Millam, M. Klene, J.E. Knox, J.B. Cross, V. Bakken, C. Adamo, J. Jaramillo, R. Gomperts, R.E. Stratmann, O. Yazyev, A.J. Austin, R. Cammi, C. Pomelli, J.W. Ochterski, R.L. Martin, K. Morokuma, V.G. Zakrzewski, G.A. Voth, P. Salvador, J.J. Dannenberg, S. Dapprich, A.D. Daniels, Farkas, J.B. Foresman, J.V. Ortiz, J. Cioslowski, D.J. Fox, Gaussian09 Revision D.01, Gaussian Inc. Wallingford CT, Gaussian 09 Revis. C.01, Gaussian Inc., Wallingford CT, 2010, <https://doi.org/10.1017/CBO9781107415324.004>.